The 4th European sCO_2 Conference for Energy Systems
March 23-24, 2021, Online Conference

2021-sCO2.eu-142

Characterizing and modelling turbulence in supercritical fluids

R. Pecnik[1], J. Ren[2] and G.J. Otero-R.[1]
(r.pecnik@tudelft.nl)

[1] *Delft University of Technology, Leeghwaterstraat 39, 2613 CB Delft, The Netherlands*
[2] *University of Nottingham, University Park, Nottingham, NG7 2RD UK*

ABSTRACT

From concentrated solar power plants to rocket engines, energy conversion systems are continually reengineered to perform ever better. Often this involves fluids being pushed into the supercritical region, where highly non-ideal thermodynamic effects are at play. Yet, our fundamental understanding of flow physics at such conditions lags behind to successfully realize these exciting engineering applications. Especially, the sharp variations in all thermophysical properties close to the critical point and the high optical density at supercritical pressures lead to significantly richer flow physics and even more intricate phenomena in turbulence. In this talk we will present our recent fundamental on turbulence in supercritical fluids, which are relevant in all component of a supercritical power cycle. We will elucidate how and when flows with supercritical fluids transition to turbulence and how compressible effects can be characterized and modelled for turbulent heat transfer.

INTRODUCTION

The continuous demand to increase the efficiency of energy conversion systems and the productivity of process plants forces engineers and scientists to use fluids at increasingly higher pressures and temperatures. For instance, to increase the thermal efficiency of power plants, engineers are currently developing a thermodynamic power cycle that operates with carbon dioxide in the supercritical region, at pressures and temperatures high enough to exceed the critical point where fluids behave in a highly non-ideal way. Such a power cycle has the potential to enable a break-through of cost-competitive, utility-scale solar thermal power plants. Another example where pressures and temperatures of fluids continuously increase is in the development of more powerful rocket engines. The idea of engineers is to use rocket fuels at supercritical conditions not only to increase fuel mixing with the oxidizer but also to cool the rocket engine using the fuel before it is injected into the combustion chamber. While cooling the rocket nozzle, the fuel is heated from initially cryogenic conditions into the supercritical region. The net result is a rocket engine that provides higher specific thrust, enabling space access with increasingly higher payloads.

One of the major obstacles in successfully realizing these technologies is the limited knowledge of turbulence in the supercritical fluid region, especially when flows are heated or cooled across the Widom line (see black dotted line in figure Figure (1)) in the supercritical region. The sharp variations in all thermophysical properties in the vicinity of the Widom line lead to significantly richer flow physics and even more intricate phenomena in turbulence.

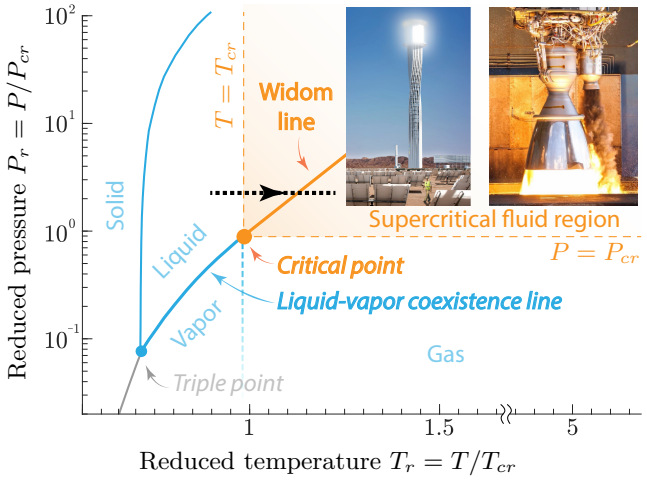

Figure 1: Pressure – temperature phase diagram of an arbitrary substance indicating the thermodynamic critical point and the supercritical fluid region. P_{cr} and T_{cr} are critical pressure and temperature, respectively. Two applications are shown which will operate in the supercritical regime.

In this paper we will discuss three topics related to flows in the supercritical fluid region. In the first topic we will discuss **boundary layer instability** with fluids in the vicinity of the critical point, where we will identify the range of disturbances to which a given laminar base flow is unstable and how these instabilities can trigger the development of turbulence. In the second topic we will discuss how **fully developed turbulent flows** with highly non-ideal fluids can distinctively be characterized by the semi-local Reynolds number and a scaling approach we proposed recently in Ref. [1]. In the third topic we will show how this scaling approach can be used to properly sensitize common **turbulence models** to account for the "leading-order effect" of variable properties on wall bounded turbulence.

DOI: 10.17185/duepublico/73973

TRANSITION TO TURBULENCE

Most of the present knowledge on stability and laminar-turbulent transition is limited to ideal gases [3] or incompressible flows, where thermodynamic properties are constant. On the other hand, numerical simulations of real gas effects (high-temperature chemical effects) in hypersonic flows has just gone through an initial stage [6, 7, 8]. These effects, often referred to as real-gas effects, include vibrational excitation, dissociation and recombination of gas species, ionization, radiation and surface ablation. Apart from the high-temperature chemical effects, stratifications in thermodynamic or/and transport properties can substantially influence the stability (see review by Govindarajan & Sahu [9], and references therein). These stratifications exist both naturally (e.g. in the Earth's outer core) and artificially (e.g. exert wall heating/cooling), revealing some of the non-ideal-gas effects.

We recently investigated the stability of boundary layer flows with fluids close to the critical point [10], through linear stability theory [11], direct numerical simulation and inviscid analysis. To account for the full non-ideal gas effects, one must take the non-ideal equation-of-state into consideration as well as the complicated functions of thermodynamic/transport properties in terms of its thermodynamic state, which can be determined by two independent thermodynamic quantities (such as density and internal energy). We study boundary layer flows with carbon dioxide (CO2) at a constant pressure of 80 bar, which is above the critical pressure (73.9 bar). The flow conditions are such chosen that different thermodynamic regimes of interests shall be well revealed.

If a fluid at constant supercritical pressure is heated, such that the Widom line is crossed (see black dotted line in figure Figure (1)), highly non-ideal effects are at play. In the vicinity of the Widom line, which is an extension of the liquid-vapor coexistence line into the supercritical fluid regime (see solid orange line in figure Figure (1)), a seemingly continuous phase transition from a compressible liquid to a dense vapor occurs with large changes in all thermophysical properties [12, 13, 14]. As the temperature at the wall increases towards the Widom line (due to viscous heating), the stability of the flow increases significantly (see neutral stability curves in the right column of figure Figure (2) (a,b) for two different Mach numbers). By crossing the Widom line, figure Figure (2)(c), a novel and peculiar second mode (Mode II) appears which overlaps with Mode I. Until now, such a phenomenon has not been observed and further research is required to unveil this intriguing mechanisms using advanced theory, comprehensive simulations and novel experiments.

To characterise the boundary layer flow we use the Reynolds number, Re_∞, Prandtl number, Pr_∞, Eckert number, Ec_∞ and the Mach number, Ma_∞ (all based on freestream parameters) which are given as:

$$Re_\infty = \frac{\rho^*_\infty u^*_\infty l^*_0}{\mu^*_\infty},\ Pr_\infty = \frac{\mu^*_\infty C^*_{p\infty}}{\kappa^*_\infty},$$

$$Ec_\infty = \frac{u^{*2}_\infty}{C^*_{p\infty} T^*_\infty},\ Ma_\infty = \frac{u^*_\infty}{a^*_\infty}. \qquad (1)$$

The subscript ∞ denotes freestream values, superscript $*$ stands for dimensional variables, l^*_0 is a chosen length scale, a^*_∞ is the speed of sound in the freestream. Note that for an ideal gas $Ec_\infty = (\gamma - 1)Ma^2_\infty$, where γ is the heat capacity ratio. In linear stability theory, l^*_0 is chosen to be the local boundary layer thickness scale δ^*,

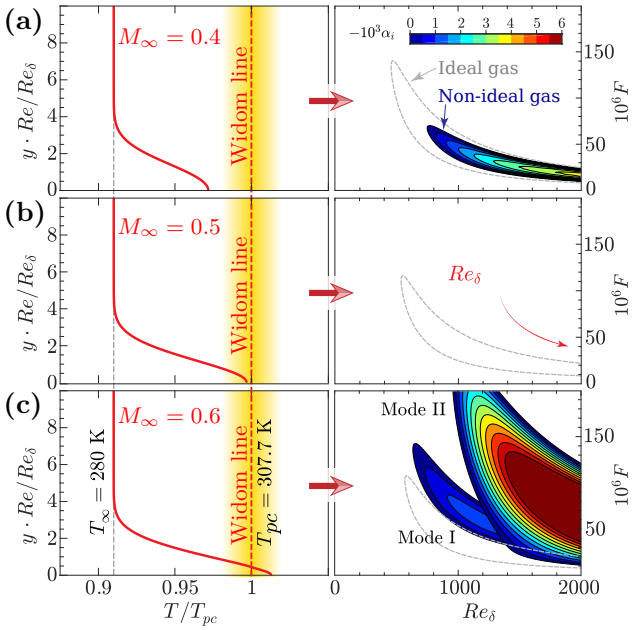

Figure 2: Boundary layer temperature profiles (left column) and corresponding neutral stability curves as function of Reynolds number, Re_δ, and perturbation frequency, F, (right column) for cases with increasing free stream Mach number ($M_\infty = [0.4, 0.5, 0.6]$). The equivalent ideal gas solution is shown in gray to highlight differences. The wall is adiabatic and the free stream temperature is at 280 K.

which results in the definition of Re_δ:

$$\delta^* = \left(\frac{\mu^*_\infty x^*}{\rho^*_\infty u^*_\infty}\right)^{1/2},$$

$$Re_\delta = \frac{\rho^*_\infty u^*_\infty \delta^*}{\mu^*_\infty} = \left(\frac{\rho^*_\infty u^*_\infty x^*}{\mu^*_\infty}\right)^{1/2}. \qquad (2)$$

Besides the known stabilization of compressibility effects (increase Ec_∞), the boundary layer flow is further stabilized by non-ideal gas effects in the subcritical or supercritical regime. In either regime, the temperature profile remains below or above T^*_{pc}, the stabilization is more prominent when T^*_∞ is closer to T^*_{pc} and/or Ec_∞ is increased.

The most interesting results lie in the transcritical regime, where the temperature profile crosses the pseudo-critical point ($T_{\rm pc} = 307.7$ K). We show in figure Figure (3) a detailed evolution of the growth rate with $T_\infty = 280$ K by gradually increasing the Eckert number afrom $Ec_\infty = 0.11$ to $Ec_\infty = 0.202$, such that the insulated wall temperature increases. Figure Figure (3)(a,b) shows the neutral curve of Mode I, while in figure Figure (3)(c) we show Mode II that becomes unstable at $Ec_\infty \geq 0.19$. It appears that the maximum critical Reynolds number Re_δ occurs at $Ec_\infty = 0.16$. The flow enters the transcritical regime (the temperature crosses the pseudo-critical point) at $Ec_\infty \geq 0.17$, and the growth rate and the extent of the neutral curve of Mode I again increases. Figure Figure (3)(b) shows the evolution of Mode I in the transcritical regime. With an increase in Ec_∞, the range of unstable Re_δ decreases, while the range for unstable F increases. Most noteworthy is the growth rate of Mode II, which increases much faster with Ec_∞ and becomes much larger than Mode I. This indicates that the flow in the transcritical regime is

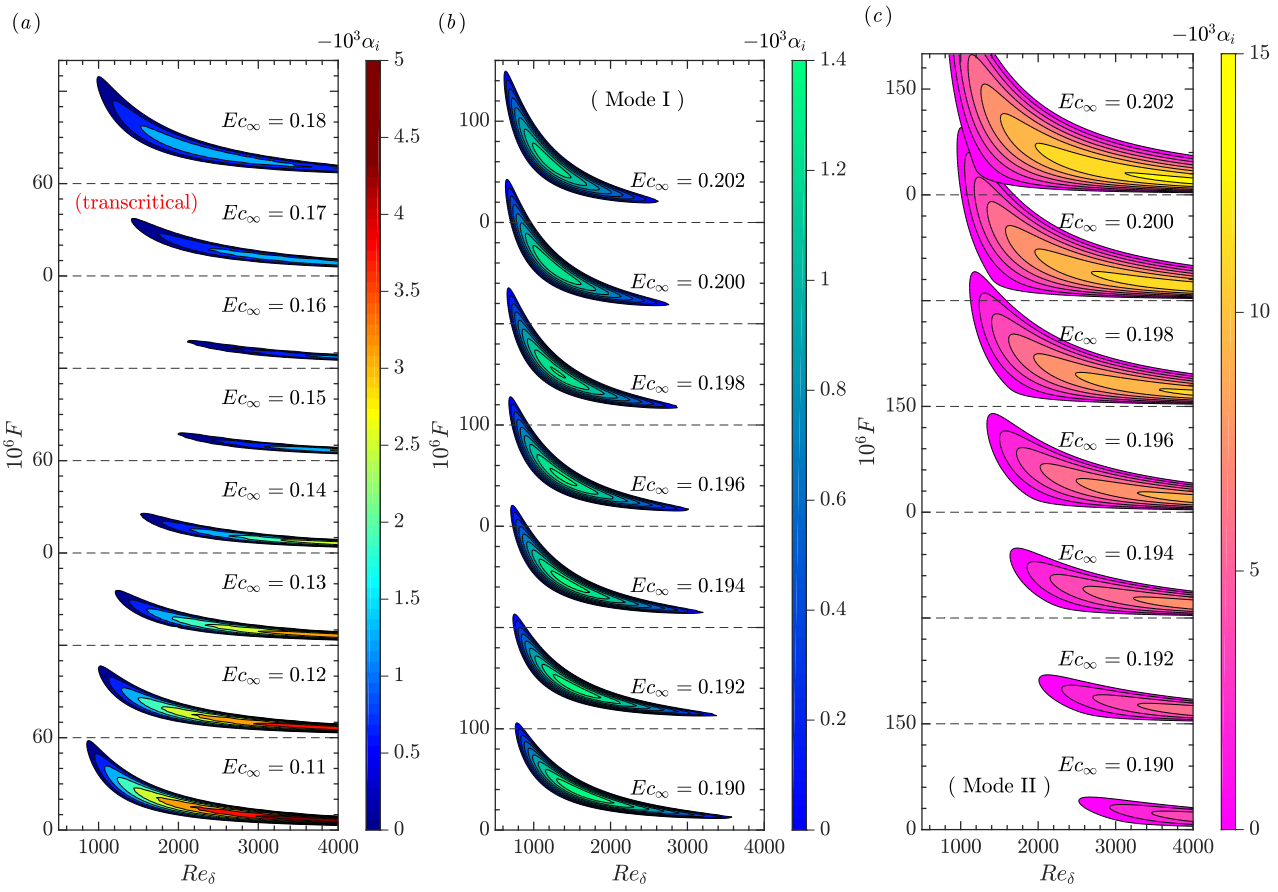

Figure 3: Growth rates of perturbations in the $F - Re_\delta$ stability diagram with $T^*_\infty = 280$ K. (a) $Ec_\infty = 0.11,\ 0.12, ..., 0.19$, (b) $Ec_\infty = 0.194,\ 0.196, ..., 0.202$.

significantly destabilized by non-ideal gas effects through Mode II.

The inviscid analysis shows that in the transcritical regime, Mode II is not caused by the trapped acoustic waves which is deemed to give rise to higher modes in hypersonic flows. We show that the generalized inflection point criterion expressed in density $D(\rho_0 D U_0)$ is valid for non-ideal gases. As result, an inviscid mechanism is present in the trans- and supercritical regimes in contrast to the subcritical regime which contains the viscous instability only.

FULLY TURBULENT FLOWS

Figure (4) shows three turbulent channel flow simulations using DNS. The fluid is volumetrically heated, while the temperature at the wall is kept at a constant value. Different constitutive relations for density, ρ, and viscosity, μ, as a function of temperature, T, were used. The case $\mathrm{CRe}^\star_\tau$ (figure (a)) corresponds to a flow for which density and viscosity are decreasing away from the wall, such that the semi-local Reynolds number $\mathrm{Re}^\star_\tau$ is constant across the whole channel height. The semi-local Reynolds number is defined as

$$Re^\star_\tau \equiv \frac{\sqrt{\langle\rho\rangle / \rho_w}}{\langle\mu\rangle / \mu_w} Re_\tau, \qquad (3)$$

where $\langle\cdot\rangle$ denotes Reynolds averaging, the subscript w indicates quantities at the isothermal wall (no averaging at the wall is required), $Re_\tau = \rho_w u_{\tau w} h/\mu_w$ is the friction Reynolds number based on friction velocity, u_{τ_w}, and a characteristic length, h. Although this case has arbitrary

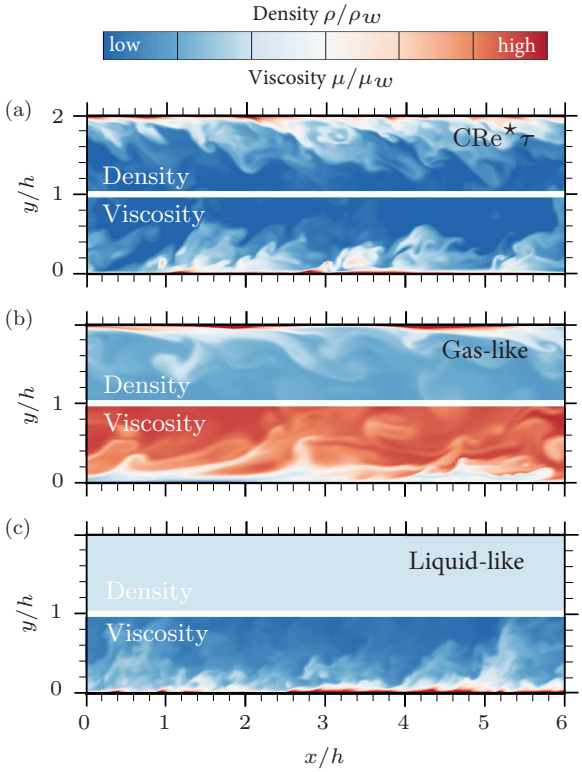

Figure 4: Contour plots of instantaneous density ρ (top half) and dynamic viscosity μ (lower half) for cases $\mathrm{CRe}^\star_\tau$ (a), Gas-like (b), and Liquid-like (c).

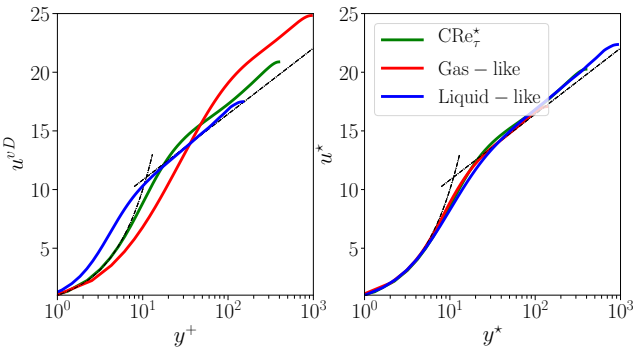

Figure 5: Contour plots of instantaneous density ρ (top half) and dynamic viscosity μ (lower half) for cases CRe$^\star_\tau$ (a), Gas-like (b), and Liquid-like (c).

thermophysical properties, it is worthwhile to mention that it bears similarities to supercritical fluids, for which both density and viscosity decrease when heated across the pseudo-critical temperature [15, 16]. The cases GL and LL (figure (b) and (c)) are flows with gas-like and liquid-like property variations that both have large gradients in $Re^\star_\tau$. More details on the governing equations, the numerical scheme and the DNS cases can be found in [1].

The streamwise velocity profiles are shown in Figure (5). Note, the van Driest velocity transformation (left figure), which is defined as $u^{vD} = \int \sqrt{\langle\rho\rangle/\rho_w}\, d(\langle u\rangle/u_{\tau_w})$, is not capable to provide a collapse for the velocity profiles of these three DNS cases. On the other hand, the velocity scaling as proposed by [17], and later independently derived by [18], provides a good collapse for all cases (right figure). The $u^\star$-velocity scaling based on the semi-local Reynolds number is expressed as,

$$u^\star = \int_0^{\overline{u}^{vD}} \left(1 + \frac{y}{Re^\star_\tau}\frac{dRe^\star_\tau}{dy}\right) d\left\langle u^{vD}\right\rangle. \qquad (4)$$

This transformation has been obtained by scaling the Navier-Stokes equation using semi-local scales, which is the key to account for the leading-order effect of variation in thermophysical properties on turbulence. This semi-local scaling approach provides a framework to collapse other turbulence properties as well and consequently provides insight to properly models turbulence as discussed in the next section.

TURBULLENCE MODELING

Common turbulence models for solving the Reynolds-averaged Navier-Stokes (RANS) equations do not correctly account for variations in thermodynamic/transport properties, such as density and viscosity, which can cause substantial inaccuracies in predicting important quantities of interest, for example, heat transfer and drag. RANS equations with simple extensions of eddy viscosity models (EVM) are currently used to predict turbulence in supercritical fluids. For example, if the turbulent kinetic energy (TKE) equation is derived on the basis of the compressible Navier-Stokes equations, additional terms appear, i.e. pressure -work and -dilatation, dilatational dissipation, and additional terms related to fluctuations of density, velocity, pressure, etc. The modification of the TKE in flows with strong heat transfer has been attributed to these terms and according models have been proposed in the past [19, 20, 21]. A different approach to sensitize turbulence models for compressible flows with large density variations, was proposed by Catris and Aupoix [22]. They used the formulation developed by Huang *et al.* [23] for the closure coefficients, to modify the diffusion term of the turbulent dissipation transport equation. Additionally, they argued that the diffusion of TKE acts upon the energy per unit volume $[(kg\ m^2/s^2)/m^3]$ of turbulent fluctuations, which can be expressed as ρk. The diffusion of TKE is therefore based on ρk, while the diffusion coefficient is divided by the density on the basis of dimensional consistency.

Based on the semi-locally scaled turbulent kinetic energy equation, introduced in [1], we analytically derive a modification of the diffusion term of turbulent scalar equations to improve the prediction of eddy viscosity models for wall-bounded turbulent flows with strong gradients in the thermo-physical properties. The modifications are based on the fact that the "leading-order effect" of variable properties on wall bounded turbulence can be characterized by the semi-local Reynolds number only [18]. For instance, the modified TKE equation reads (averaging operators omitted),

$$\frac{\partial\rho k}{\partial t} + \frac{\partial\rho k u_j}{\partial x_j} = P_k - \rho\varepsilon + \frac{1}{\sqrt{\rho}}\frac{\partial}{\partial x_j}\left[\frac{1}{\sqrt{\rho}}\left(\mu + \frac{\mu_t}{\sigma_k}\right)\frac{\partial\rho k}{\partial x_j}\right]. \qquad (5)$$

If compared to the conventional model for the TKE, the newly derived equation shows only one major difference that lies in the diffusion term. The diffusion term that emerges from the semi-local scaling methodology is a function of ρk (instead of k), while the diffusion coefficient and the overall diffusion term are divided by $\sqrt{\rho}$. This is similar to the density corrections proposed by [22], except that in [22], only the diffusion coefficient is divided by ρ.

The developed methodology is generic and applicable to a wide range of eddy viscosity models. We have applied the same methodology to several turbulent scalars (ε, ω, among others) of common eddy viscosity models: the eddy viscosity correlation of Cess [24], the one-equation model of Spalart Allmaras (SA) [25], the low Reynolds number $k-\varepsilon$ model of Myong and Kasagi (MK) [26], Menter's shear stress transport model (SST) [27], and the four-equations v^2-f model (V2F) [28]. An additional modification we have introduced is to replace y^+ and Re_τ, e.g. within the eddy viscosity correlation of Cess and for the damping function of the MK turbulence model, by their semi-local counterparts, namely $y^\star$ and $Re^\star_\tau$ [1].

We have tested the EVM to available direct numerical simulations (DNS) of volumetrically heated fully developed turbulent channel flows with varying thermophysical properties which have been introduced earlier. The density and the viscosity are a function of temperature and different constitutive relations are used, that resemble behaviours of liquids (LL), gases (GL), supersonic fluids (SS), and fluids close to the vapour-critical point (C$Re^\star_\tau$).

The results are reported in Figure (6) in terms of $u^\star$ (see equation (4)) and u^{vD}, which is the van Driest velocity transformation. The modifications clearly improve the EVM for flows with strong variations on the thermophysical properties. A substantial improvement is seen in Cess and the MK model; the damping function of these modified models is able to correctly account for variations of transport properties. Interestingly, the original SA model, originally developed for external flow, gives

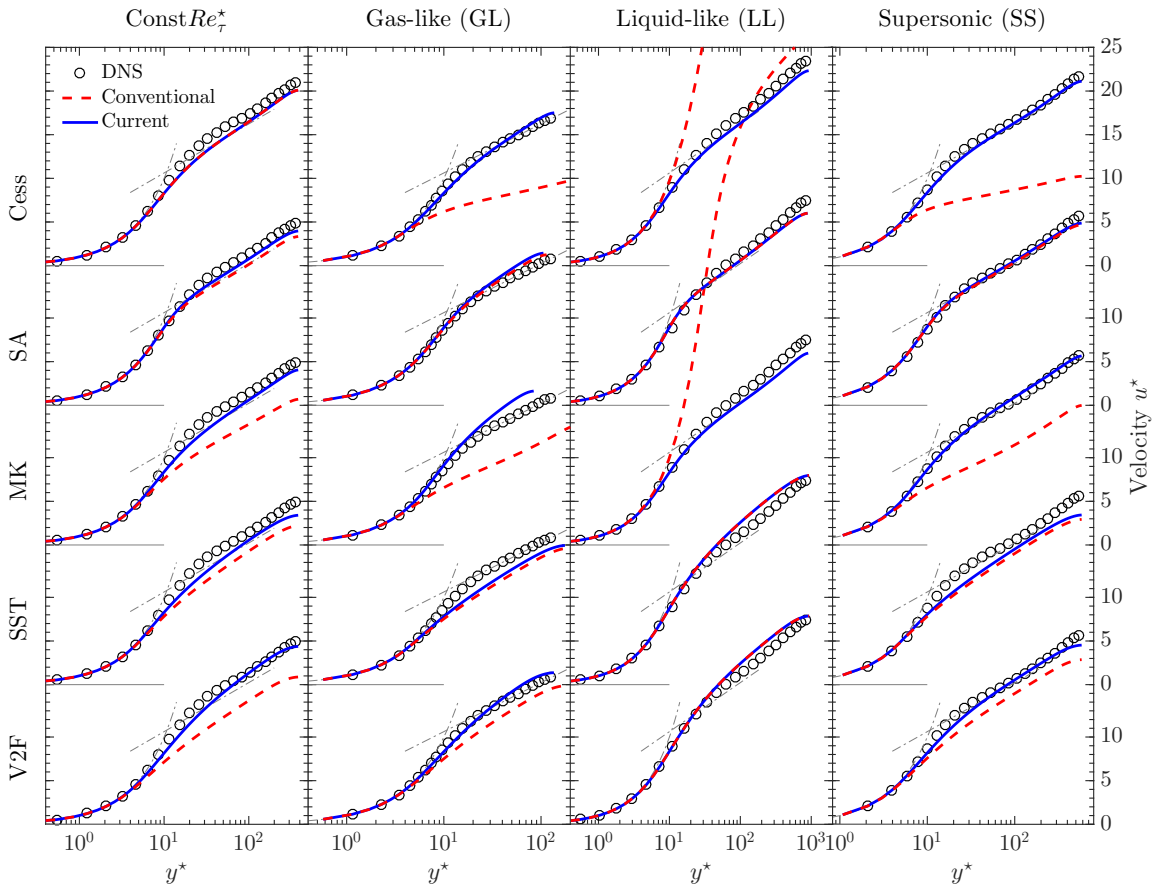

Figure 6: Universal velocity transformation $u^\star$ with respect to the semi-locally scaled wall normal distance $y^\star$ for a fully developed turbulent channel. The grey dashed lines represent $u^\star = y^\star$ and $u^\star = 1/\kappa\ ln(y^\star) + C$, the viscous sublayer and log-law region, respectively, where $C = 5.5$.

the most reliable results, with respect to other conventional EVM, for the cases studied. For the modified SST model, the performance with respect to the universal law of the wall is not satisfactory. The modified V2F formulation improves the collapse with the DNS data if compared to the conventional form for all the cases. For the profile of $u^\star$, a good collapse is seen with the DNS data for most of the modified EVM, outperforming the original models.

CONCLUSION

Several conclusions can be drawn on the topics discussed in this paper, which are separately discussed hereafter.

Boundary layer stability The compressibility effects close to the critical point strongly stabilise the boundary layer. Using modal stability analysis we showed that for conditions where the free-stream temperature is below the pseudo-critical point, the maximum boundary layer stabilisation is achieved when the temperature at the wall increase towards the Widom line. Once the temperature at the wall crosses the Widom line, due to an increase in Mach number, a novel instability mode appears. The growth rate of this mode increases much faster with Ec_∞ and becomes much larger than Mode I. This indicates that the flow in the transcritical regime is significantly destabilised by non-ideal gas effects.

Fully developed turbulent flows We have recently derived a simple scaling transformation of the Navier-Stokes equations using semi-local quantities, which allows to account for the "leading order effect" of variable properties on turbulence. One outcome of this approach is a velocity transformation that allows to collapse velocity profiles for channel flows with arbitrary variations in density and viscosity.

Turbulence modelling Based on the semi-local scaling framework we have also derived a novel methodology to improve eddy viscosity models for predicting wall-bounded turbulent flows with strong variations in thermo-physical properties. The major difference of the new methodology is the formulation of the diffusion term in the turbulence scalar equations. The conclusion is that the diffusion of turbulent kinetic energy acts upon the energy per unit volume and not per unit mass. In general, the modified EVMs result in a much better agreement with the DNS data in terms of velocity profiles and heat transfer of fully developed turbulent channel flows with variable property fluids. The next step in modelling turbulence should focus on effects related to very large density fluctuations (larger than the ones considered herein) and to turbulence deterioration emerging from flow acceleration and buoyancy forces.

REFERENCES

[1] R. Pecnik and A. Patel, "Scaling and modelling of turbulence in variable property channel flows," *Journal of Fluid Mechanics*, vol. 823, no. R1, 2017.

[2] A. Sameen and R. Govindarajan, "The effect of wall heating on instability of channel flow," *Journal of Fluid Mechanics*, vol. 577, pp. 417–442, 2007.

[3] A. Fedorov, "Transition and stability of high-speed boundary layers," *Annual Review of Fluid Mechanics*, vol. 43, no. 1, pp. 79–95, 2011.

[4] L. M. Mack, "Boundary-layer linear stability theory," in *AGARD Report No. 709 Special Course on Stability and Transition of Laminar Flow*, 1984.

[5] S. Kawai, "Direct numerical simulation of transcritical turbulent boundary layers at supercritical pressures with strong real fluid effects," in *54th AIAA Aerospace Sciences Meeting*, p. 1934, 2016.

[6] X. Zhong and X. Wang, "Direct numerical simulation on the receptivity, instability, and transition of hypersonic boundary layers," *Annual Review of Fluid Mechanics*, vol. 44, no. 1, pp. 527–561, 2012.

[7] O. Marxen, T. E. Magin, E. S. Shaqfeh, and G. Iaccarino, "A method for the direct numerical simulation of hypersonic boundary-layer instability with finite-rate chemistry," *Journal of Computational Physics*, vol. 255, pp. 572–589, 2013.

[8] O. Marxen, G. Iaccarino, and T. E. Magin, "Direct numerical simulations of hypersonic boundary-layer transition with finite-rate chemistry," *Journal of Fluid Mechanics*, vol. 755, pp. 35–49, 2014.

[9] R. Govindarajan and K. C. Sahu, "Instabilities in viscosity-stratified flow," *Annual Review of Fluid Mechanics*, vol. 46, pp. 331–353, 2014.

[10] J. Ren, O. Marxen, and R. Pecnik, "Boundary-layer stability of supercritical fluids in the vicinity of the widom line," *Journal of Fluid Mechanics*, vol. 871, pp. 831–864, 2019.

[11] J. Ren, S. Fu, and R. Pecnik, "Linear instability of poiseuille flows with highly non-ideal fluids," *Journal of Fluid Mechanics*, vol. 859, pp. 89–125, 2019.

[12] G. G. Simeoni, T. Bryk, F. A. Gorelli, M. Krisch, G. Ruocco, M. Santoro, and T. Scopigno, "The Widom line as the crossover between liquid–like and gas–like behaviour in supercritical fluids," *Nature Physics*, vol. 6, pp. 503–507, 2010.

[13] D. Bolmatov, V. V. Brazhkin, and K. Trachenko, "Thermodynamic behaviour of supercritical matter," *Nature Communications*, vol. 4, pp. 1–7, 2013.

[14] D. Banuti, "Crossing the widom-line – supercritical pseudo-boiling," *The Journal of Supercritical Fluids*, vol. 98, pp. 12 – 16, 2015.

[15] J. W. Peeters, R. Pecnik, M. Rohde, T. van der Hagen, and B. Boersma, "Turbulence attenuation in simultaneously heated and cooled annular flows at supercritical pressure," *Journal of Fluid Mechanics*, vol. 799, pp. 505–540, 2016.

[16] H. Nemati, A. Patel, B. J. Boersma, and R. Pecnik, "The effect of thermal boundary conditions on forced convection heat transfer to fluids at supercritical pressure," *Journal of Fluid Mechanics*, vol. 800, pp. 531–556, 2016.

[17] A. Trettel and J. Larsson, "Mean velocity scaling for compressible wall turbulence with heat transfer," *Physics of Fluids*, vol. 28, no. 2, p. 026102, 2016.

[18] A. Patel, B. Boersma, and R. Pecnik, "The influence of near-wall density and viscosity gradients on turbulence in channel flows," *Journal of Fluid Mechanics*, vol. 809, pp. 793–820, 2016.

[19] P. G. Huang, P. Bradshaw, and T. J. Coakely, "Turbulence models for compressible boundary layers," *AIAA Journal*, vol. 32, no. 4, pp. 735–740, 1994.

[20] S. Sarkar, G. Erlebacher, M. Hussaini, and H. Kreiss, "The analysis and modelling of dilatational terms in compressible turbulence," *Journal of Fluid Mechanics*, vol. 227, pp. 473–493, 1991.

[21] O. Zeman, "A new model for super/hypersonic turbulent boundary layers," in *31st Aerospace Sciences Meeting*, p. 897, 1993.

[22] S. Catris and B. Aupoix, "Density corrections for turbulence models," *Aerospace Science and Technology*, vol. 4, no. 1, pp. 1–11, 2000.

[23] P. Huang, P. G., Coleman, G. N., Bradshaw, "Compressible Turbulent channel flows, DNS results and modelling," *JFM*, no. 1995, pp. 185–218, 1995.

[24] R. Cess, "A survey of the literature on heat transfer in turbulent tube flow," *Res. Rep*, pp. 8–0529, 1958.

[25] P. R. Spalart, S. R. Allmaras, *et al.*, "A one equation turbulence model for aerodynamic flows," *RECHERCHE AEROSPATIALE-FRENCH EDITION-*, pp. 5–5, 1994.

[26] N. Myong, H.K. and Kasagi, "A New Approach to the Improvement of k-e turbulence model for wall-bounded shear flows," *JSME*, vol. 33, no. 2, 1990.

[27] F. R. Menter, "Zonal Two Equation k-w, Turbulence Models for Aerodynamic Flows," *AIAA paper*, p. 2906, 1993.

[28] P. A. Durbin, "Separated Flow Computations with the k-e-v2 Model," *AIAA Journal*, vol. 33, no. 4, pp. 659–664, 1995.

DuEPublico

Duisburg-Essen Publications online

UNIVERSITÄT DUISBURG ESSEN

Offen im Denken

ub | universitäts bibliothek

Published in: 4th European sCO2 Conference for Energy Systems, 2021

This text is made available via DuEPublico, the institutional repository of the University of Duisburg-Essen. This version may eventually differ from another version distributed by a commercial publisher.

DOI: 10.17185/duepublico/73973
URN: urn:nbn:de:hbz:464-20210330-115710-0

This work may be used under a Creative Commons Attribution 4.0 License (CC BY 4.0).